Published in final edited form as:
Methods Mol Biol. 2010 ; 587: 45–56. doi:10.1007/978-1-60327-355-8_4.

Kinetics of Motor Protein Translocation on Single Stranded DNA

Christopher J. Fischer[1], **Lake Wooten**[1], **Eric J. Tomko**[2], and **Timothy M. Lohman**[2]
[1]Department of Physics and Astronomy, University of Kansas, 1251 Wescoe Hall Dr., 1082 Malott Hall, Lawrence, KS 66045 USA

[2]Department of Biochemistry and Molecular Biophysics, Washington University School of Medicine, 660 S. Euclid Avenue, Box 8231, St. Louis, MO 63110 USA

Abstract

The translocation of nucleic acid motor proteins along DNA or RNA can be studied in ensemble experiments by monitoring either the kinetics of the arrival of the protein at a specific site on the nucleic acid filament (generally one end of the filament) or the kinetics of ATP hydrolysis by the motor protein during translocation. The pre-steady state kinetic data collected in ensemble experiments can be analyzed by simultaneous global non-linear least squares (NLLS) analysis using a simple sequential "*n-step*" mechanism to obtain estimates of the rate-limiting step(s) in the translocation cycle, the average "kinetic step-size", and efficiency of coupling ATP binding and hydrolysis to translocation.

Keywords

translocase; kinetics; ATPase; helicase; motor protein

1. Introduction

The ability to translocate processively and with biased directionality along a nucleic acid filament is central to the biological function of several enzymes including polymerases (1), helicases (2–4), chromatin remodelers (5, 6), some nucleases (7, 8) and some restriction enzymes (9–11). These "molecular motors" all use the chemical potential energy obtained through the binding and hydrolysis of nucleoside triphosphates (NTP or dNTP) to perform the mechanical work of directional translocation along the filament. An understanding of the translocation mechanisms of these motor proteins requires quantitative kinetic information to obtain the rate constants, processivities, kinetic step-sizes, and ATP coupling stoichiometries associated with translocation. Here, we describe the use and analysis of pre-steady state ensemble kinetic approaches (3, 6, 10–17) to probe the translocation mechanisms of processive translocases along nucleic acids using a simple sequential "*n-step*" kinetic model. The application of this methodology provides an accurate determination of macroscopic kinetic parameters such as the rate of net forward motion of the translocase along the nucleic acid and the net efficiency at which the hydrolysis of ATP is coupled to this net forward motion. However, the estimates of microscopic kinetic parameters, such as the kinetic step size of translocation, can be inflated under some circumstances if non-uniform motion occurs during translocation.

Correspondence to: Christopher J. Fischer; Timothy M. Lohman.

2. Materials

2.1 Matching Experimental Conditions to Model Assumptions

The kinetic model and associated equations used here assume that no more than one translocase is bound to each nucleic acid. Thus, the application of these equations to the analysis of kinetic data requires that the experiments are performed under conditions that favor this binding distribution; this is generally achieved by performing the experiments under conditions where the concentration of the nucleic acid is in excess of the concentration of the translocase. This model also assumes that any translocase that is initially free in solution at the start of the reaction or that dissociates from the nucleic acid during translocation is prevented from rebinding to the nucleic acid. This is accomplished experimentally by including a protein trap. When selecting such a trap it is best to use one that does not stimulate the ATPase activity of the translocase (18). This will allow for more straightforward and simple analysis of the ATPase activity of the translocase that is associated with translocation.

3. Methods

3.1 Mathematical Model for Translocation

The sequential "n-step" kinetic mechanism shown in Scheme 1 has been used to model helicase translocation and its coupling to ATP hydrolysis (13, 18). In this mechanism (13), depicted in Figure 1, a translocase with an occluded site size of b nucleotides and a contact size of d nucleotides binds with polarity to a nucleic acid filament, L nucleotides long. The contact size, d, represents the number of consecutive nucleotides required to satisfy all contacts with the translocase and is thus less than or equal to the occluded site size. In this discussion we will assume that translocation along the nucleic acid is directionally biased from 3' to 5', but the results are equally applicable to a translocase which exhibits the opposite directional bias.

The translocase is initially bound i translocation steps away from the 5'-end, with concentration, I_i. The number of translocation steps, i, is constrained ($1 \leq i \leq n$), where n is the maximum number of translocation steps needed for a translocase bound initially at the 3' end to move to the 5' end of the nucleic acid. In the discussion here we considered two initial binding states for the translocase: one in which all proteins initiate translocation from the same site on the nucleic acid (in this case at the 3' end of the nucleic acid, which is n steps away from the 5' end) and one in which the proteins initiate translocation from random binding sites on the nucleic acid.

Upon addition of ATP the translocase moves with directional bias along the nucleic acid via a series of repeated rate-limiting translocation steps each associated with the same rate constant, k_t. The rate constant for protein dissociation during translocation is k_d. The processivity of translocation along the nucleic acid is thus defined as $P=\frac{k_t}{k_d+k_t}$. Between two successive rate-limiting translocation steps the enzyme moves m nucleotides, while hydrolyzing c ATP molecules. Therefore, c/m is defined as the macroscopic ATP coupling stoichiometry and corresponds to the average number of ATP molecules hydrolyzed per nucleotide translocated along the nucleic acid. Similarly the product mk_t is the macroscopic translocation rate in units of nt/s. When the translocase reaches the 5'-end of the nucleic acid it continues to hydrolyze ATP with rate constant k_a and dissociates from the nucleic acid with rate constant k_{end}. This hydrolysis of ATP at the end of the nucleic acid is not coupled to the physical movement of the enzyme along the nucleic acid and thus is referred to as futile hydrolysis (18, 19).

We note that, in general, k_t represents the rate constant for the rate-limiting step that occurs within each repeated translocation cycle and does not necessarily correspond to the rate constant for physical movement of the translocase along the nucleic acid (13). Similarly, the average number of nucleotides translocated between two successive rate-limiting steps, defined as the translocation "kinetic step-size" (m), can be larger than the length of nucleic acid traversed during hydrolysis of a single ATP.

Based on Scheme 1, the expressions in Equations (1) and (4) can be derived (13, 16) for the time-dependent accumulation of protein at the 5' end of the nucleic acid. In these equations, L^{-1} is the inverse Laplace transform operator, s is the Laplace variable (16) and the parameters k_t, k_d, k_{end}, c, k_a and n are as defined above and r is the initial (at time, t = 0) ratio of the probability of the translocase binding to any one binding position on the nucleic acid other than the 5' end to the probability of the translocase binding to the 5' end (13, 14). For the case where all the proteins are initially bound at the same position (in this case taken to be the 3' end of the nucleic acid), the equation for the time-dependent accumulation of protein at the 5' end of the nucleic acid is given by Equation (1).

$$f_{5'}(t)=A^{*}L^{-1}\left[\frac{1}{k_{end}+s}\left(\frac{k_t}{k_t+k_d+s}\right)^{n}\right] \quad (1)$$

For the case where all the proteins are initially bound at random positions along the nucleic acid, the equation for the time-dependent accumulation of protein at the 5' end of the nucleic acid is given by Equation (2).

$$f_{5'}(t)=\frac{A}{1+n^{*}r}L^{-1}\left[\frac{1}{s+k_{end}}*\left(1+\frac{k_t{}^{*}r}{s+k_d}\left(1-\left(\frac{k_t}{s+k_t+k_d}\right)^{n}\right)\right)\right] \quad (2)$$

The scalar A in Equations (1) and (2) allows for conversion of the concentration of protein bound at the 5' end of the nucleic acid into a signal that can be measured experimentally (*e.g.*, a spectroscopic change) (13, 14, 18).

Similarly, Equations (3) and (4) are expressions for the time-dependent production of ADP or P_i, due to ATP hydrolysis by the translocases (13). In Equations (3) and (4), $I(0)$ is the concentration of translocase initially bound to the nucleic acid (at time, t =0). Equation (3) describes the ATP production occurring when all proteins are initially bound at the same position (*e.g.*, the 3' end of the nucleic acid) and Equation (4) describes the ATP production occurring when all the proteins are initially bound at random positions along the nucleic acid.

$$ADP(t)=I(0)^{*}L^{-1}\left[\frac{1}{s}\left(\frac{c^{*}k_t{}^{*}\left(1-\left(\frac{k_t}{k_t+k_d+s}\right)^{n}\right)}{k_d+s}+\frac{k_a}{k_{end}+s}\left(\frac{k_t}{k_t+k_d+s}\right)^{n}\right)\right] \quad (3)$$

$$ADP(t)=\frac{I(0)}{1+n^{*}r}L^{-1}\left[\frac{1}{s}\left(\frac{c^{*}k_t{}^{*}r^{*}\left(n(k_d+s)+k_t\left(\left(\frac{k_t}{k_t+k_d+s}\right)^{n}-1\right)\right)}{(k_d+s)^{2}}+\frac{k_a\left(1+\frac{k_t{}^{*}r\left(1-\left(\frac{k_t}{k_t+k_d+s}\right)^{n}\right)}{k_d+s}\right)}{k_{end}+s}\right)\right] \quad (4)$$

The maximum number of translocation steps, n, for a nucleic acid of a length, L, is related to the translocation kinetic step-size, m, and the translocase contact size by Equation (5).

$$n=\frac{L-d}{m} \quad (5)$$

Equation (5) can be re-expressed as Equation (6) which allows for the determination of m from the experimentally determined dependence of L on n.

$$L=mn+d \quad (6)$$

3.2 Monitoring the Kinetics of the Arrival of the Translocase at a Specific Site on the Nucleic Acid

The first experimental method we consider is a stopped-flow fluorescence approach first introduced by Dillingham *et al.*(20) and subsequently modified by Fischer et al (refs) and is depicted in Figure 2A. The method utilizes a series of oligodeoxythymidylates of varying lengths, L $(dT)_L$), that have a fluorophore attached covalently to either the 3' or 5' end of the nucleic acid. The fluorophore is chosen such that a fluorescence intensity change occurs when the translocase is bound at that end possessing the fluorophore. In this way, one can monitor the change in concentration of translocases bound at the end of the nucleic acid resulting from arrival of translocases due to translocation from other sites on the nucleic acid and dissociation of translocases from the end. Quantitative analysis of a series of these time-courses performed as a function of L using Equation (1) or (2) allows one to estimate the microscopic kinetic parameters associated with translocation of the enzyme along the nucleic acid. A subsequent estimate of the kinetic step size, m, is then obtained from the analysis of the dependence of n on L through Equation (6). We have found that Cy3 and Fluorescein have generally yielded good signal changes for the translocases that we have studied (14, 18, 21, 22).

The directionality of translocation can be determined by comparing the timecourses observed when the fluorophore is attached to the 3' versus the 5' end of the nucleic acid (13, 14, 20). Specifically, characteristic changes in the fluorescence timecourse as a function of increasing nucleic acid length (*e.g.* an increase in both the time required to reach peak fluorescence and the breadth of the fluorescence peak as shown in Figure 2A) will occur if the translocation direction is biased toward the fluorophore, but not when it is biased away from the fluorophore.

3.3 Monitoring the Kinetics of ATP Hydrolysis by the Translocase During Translocation

Enzyme translocation along nucleic acids can also be monitored by measuring the amount of ATP hydrolyzed by the enzyme during translocation. This approach requires transient pre-steady state kinetic experiments rather than steady-state ATPase experiments since steady-state rates of ATP hydrolysis will generally be limited by other kinetic processes that are slower than protein translocation (*e.g.* dissociation and/or rebinding of protein to another nucleic acid molecule). The pre-steady state rate and extent of ATP hydrolysis by the translocating protein can be monitored, for example, by directly measuring the conversion of ATP to ADP using a radioactive assay (23, 24) or by monitoring the release of inorganic phosphate using a fluorescently labeled phosphate-binding protein (18, 19) as depicted in Figure 2B.

Analysis of a series of time courses of ATP hydrolysis during translocation performed as a function of DNA length, L, can be analyzed using Equation (3) or (4) to determine estimates of the microscopic parameters c and k_a and, thus, the macroscopic ATP coupling stoichiometry c/m. In this analysis, the values of the microscopic parameters obtained from

the analysis of translocation time courses using Method 3.2 (k_t, k_d, k_{end}, m, and i) are used as fixed constraints in the application of Equations (3) or (4) (18).

4. Notes

4.1

Significant correlation exists between the parameters in Equations (1) through (4). For this reason, it is best to independently determine as many parameters as possible so that they can be constrained in the NLLS analysis using these equations. For example, the rate of dissociation during translocation (k_d in Scheme 1) can be determined independently by monitoring the dissociation of enzyme during translocation along an infinitely long nucleic acid (13, 14, 18).

4.2

It is worth noting that the presence of the fluorophore might affect the rate of translocation and/or the rate of dissociation near the fluorophore (14, 18). It is also possible that variations in the electrostatics of the nucleic acid molecule near its ends may contribute to differences in k_t and k_d at binding positions near the ends. Thus, for an enzyme that translocates in a 3' to 5' direction, the values for k_t and k_d obtained from fitting experimental time-courses obtained with nucleic acid labeled with a fluorophore at the 3' end may not equal the values of k_t and k_d that apply in the absence of the fluorophore or to interior regions of the nucleic acid. Similarly, the value of k_{end} obtained from fitting experimental time-courses obtained with nucleic acid labeled with a fluorophore at the 5' end may not equal the value of k_{end} that applies in the absence of the fluorophore (13, 18).

4.3

The model (Scheme 1) used to obtain Equations (1) through (4) assumes translocation occurs via a uniform repetition of irreversible rate-limiting steps, and ignores any non-uniformity in the translocation process. To further evaluate the efficacy of this methodology when such non-uniformity exists, we used a Monte Carlo computer simulation to generate translocation time courses for models that contained non-uniform motion as well as heterogeneity in the rates. We considered backward motion, random pausing, simple heterogeneity in the microscopic translocation rate constant (k_t) or step-size (m) for each individual kinetic step, persistent heterogeneity (25) in the microscopic translocation rate constant (k_t) or the kinetic step size (m), and repetitive shuttling of the translocase on the nucleic acid (26, 27). We note that the existence of persistent heterogeneity for the entire translocation process, commonly referred to as "static disorder" (28) could result only if each enzyme were chemically or conformationally different over the time period of the experiment. Yet, there are clear examples of such static disorder in processive nucleic acid enzymes, such as RNA polymerase (29) and some helicases (25, 30, 31). These simulated time courses were then analyzed using the simple uniform sequential n-step mechanism (Equations (1) through (6)) to obtain estimates of k_t c, and m that were then compared to the input values of these kinetic parameters.

Our analysis of these simulated data sets demonstrated that the values of the macroscopic translocation rate (mk_t) and the coupling stoichiometry (c/m) obtained using these equations reliably reflect the actual input values used for the simulations *regardless* of the presence of any non-uniform motion of the translocase. The macroscopic translocation rate is well constrained in the NLLS analysis since it is determined from the dependence on nucleic acid length of the mean arrival time of proteins at the end of the nucleic acid. Similarly, the resulting estimate of c/m provides an accurate estimate of the total ATP consumption associated with the *net forward motion* of the translocase along the nucleic acid. Intuitively

when backward motion or random pausing is introduced, the coupling stoichiometry will increase since some ATP hydrolysis results in backward motion or pausing rather than in forward motion.

The individual estimates of m and k_t are largely constrained by both the standard deviation of the distribution of arrival times of proteins at the end of the nucleic acid and the dependence of this distribution on nucleic acid length. Importantly, the inclusion of simple heterogeneity in k_t or m did not affect the estimates of mk_t, c/m, m, r, *or* k_a obtained from the analysis of the simulated time courses using equations (1) through (6). This result is significant since we believe that this simulation of simple heterogeneity is a reasonable model of the stochastic fluctuations in k_t and m that are expected for a chemically and structurally homogenous population of translocases. However, any perturbation that increases the standard deviation of the distribution of arrival times at any particular point along the nucleic acid will also increase the estimate of m obtained from the fit. Clearly, introducing backward motion, static disorder, repetitive shuttling, or random pausing will spread out the distribution of arrival times at the 5' end of the nucleic acid and will furthermore increase the dependence of the standard deviation on the length of the nucleic acid. As such, the introduction of any of these perturbations will, in fact, result in an overestimate of m. The exact amount of the overestimate will naturally depend upon the type of perturbation and its magnitude, but also on the magnitudes of the other rate constants associated with translocation since all of these variables are highly correlated in the sequential "n-step" model.

4.4

Use of the uniform sequential "n-step" model to analyze time courses obtained from experiments in which the translocase initiates at random positions along the nucleic acid requires inclusion of the r parameter in Equations (2) and (4). If the translocase has equal affinity for all potential binding sites on the nucleic acid then r must have a value between 1 and m depending upon the specific details of the translocation mechanism near the end of the nucleic acid (see (13) for more details). Thus, estimated values of r for which $r > m$ may indicate a failure of the simple model to correctly describe the translocation process, *regardless* of the quality of the fits. In other words, r can serve as an indicator of potential non-uniformity in the translocation mechanism. It is worth noting that increases in the estimate of r were associated with each of the perturbations we considered with the exception of simple heterogeneity in k_t or m. Furthermore, these increases in the estimate of r were especially large when static disorder or repetitive shuttling was incorporated into the simulations. Hence, a value of $r \gg m$ can be an indicator of non-uniformity or static disorder in the translocation kinetics.

4.5

The results of analysis of computer simulated data using Equations (1) through (4) also indicate that the presence of non-uniform motion can also increase the estimate of the rate of futile ATP hydrolysis at the end of the nucleic acid (k_a in Scheme 1). Hence the observation of futile hydrolysis at the end of the nucleic acid is also an indication that non-uniform motion may be occurring. In such a case, one should perform additional experiments or additional computer simulations to independently determine whether futile hydrolysis at the end of the nucleic acid actually occurs.

Acknowledgments

The authors thank Dr. Carsten Timm, Dr. Siyuan Han, and Dr. Matthew Antonik, Dr. Karl Maluf, Dr. Aaron Lucius, and Dr. Nathan Baker for useful discussions concerning this manuscript. This research was supported, in part, by startup funding from the University of Kansas (to C.J.F.), an University of Kansas Undergraduate Research

Award (to L.W.), and by NIH grants GM045948 (to T.M.L) and P20 RR17708 from the Institutional Development Award (IDeA) Program of the National Center for Research Resources (to C.J.F.).

References

1. Kornberg RD. The molecular basis of eukaryotic transcription. Proc Natl Acad Sci U S A. 2007; 104:12955–12961. [PubMed: 17670940]
2. Lohman TM, Bjornson KP. Mechanisms of helicase-catalyzed DNA unwinding. Annu Rev Biochem. 1996; 65:169–214. [PubMed: 8811178]
3. Lohman TM, Hsieh J, Maluf NK, Cheng W, Lucius AL, Fischer CJ, Brendza KM, Korolev S, Waksman G. Hackney DD, Tamanoi F. DNA Helicases, Motors that Move Along Nucleic Acids: Lessons from the SF1 Helicase Superfamily. The Enzymes (Third ed.). 2003
4. Matson SW, Kaiser-Rogers KA. DNA helicases. Annu Rev Biochem. 1990; 59:289–329. [PubMed: 2165383]
5. Becker PB. Nucleosome remodelers on track. Nat Struct Mol Biol. 2005; 12:732–733. [PubMed: 16142222]
6. Fischer CJ, Saha A, Cairns BR. Kinetic model for the ATP-dependent translocation of Saccharomyces cerevisiae RSC along double-stranded DNA. Biochemistry. 2007; 46:12416–12426. [PubMed: 17918861]
7. Kovall RA, Matthews BW. Structural, functional, and evolutionary relationships between lambda-exonuclease and the type II restriction endonucleases. Proc Natl Acad Sci U S A. 1998; 95:7893–7897. [PubMed: 9653111]
8. Kovall RA, Matthews BW. Type II restriction endonucleases: structural, functional and evolutionary relationships. Current opinion in chemical biology. 1999; 3:578–583. [PubMed: 10508668]
9. Szczelkun MD. Kinetic models of translocation, head-on collision, and DNA cleavage by type I restriction endonucleases. Biochemistry. 2002; 41:2067–2074. [PubMed: 11827554]
10. Firman K, Szczelkun MD. Measuring motion on DNA by the type I restriction endonuclease EcoR124I using triplex displacement. Embo J. 2000; 19:2094–2102. [PubMed: 10790375]
11. McClelland SE, Dryden DT, Szczelkun MD. Continuous assays for DNA translocation using fluorescent triplex dissociation: application to type I restriction endonucleases. J Mol Biol. 2005; 348:895–915. [PubMed: 15843021]
12. Ali JA, Lohman TM. Kinetic measurement of the step size of DNA unwinding by Escherichia coli UvrD helicase. Science. 1997; 275:377–380. [PubMed: 8994032]
13. Fischer CJ, Lohman TM. ATP-dependent translocation of proteins along single-stranded DNA: models and methods of analysis of pre-steady state kinetics. J Mol Biol. 2004; 344:1265–1286. [PubMed: 15561143]
14. Fischer CJ, Maluf NK, Lohman TM. Mechanism of ATP-dependent translocation of E.coli UvrD monomers along single-stranded DNA. J Mol Biol. 2004; 344:1287–1309. [PubMed: 15561144]
15. Lucius AL, Jason Wong C, Lohman TM. Fluorescence stopped-flow studies of single turnover kinetics of E.coli RecBCD helicase-catalyzed DNA unwinding. J Mol Biol. 2004; 339:731–750. [PubMed: 15165847]
16. Lucius AL, Maluf NK, Fischer CJ, Lohman TM. General methods for analysis of sequential "n-step" kinetic mechanisms: application to single turnover kinetics of helicase-catalyzed DNA unwinding. Biophys J. 2003; 85:2224–2239. [PubMed: 14507688]
17. Lucius AL, Vindigni A, Gregorian R, Ali JA, Taylor AF, Smith GR, Lohman TM. DNA unwinding step-size of E. coli RecBCD helicase determined from single turnover chemical quenched-flow kinetic studies. J Mol Biol. 2002; 324:409–428. [PubMed: 12445778]
18. Tomko EJ, Fischer CJ, Niedziela-Majka A, Lohman TM. A Nonuniform Stepping Mechanism for E. coli UvrD Monomer Translocation along Single-Stranded DNA. Mol Cell. 2007; 26:335–347. [PubMed: 17499041]
19. Dillingham MS, Wigley DB, Webb MR. Demonstration of unidirectional single-stranded DNA translocation by PcrA helicase: measurement of step size and translocation speed. Biochemistry. 2000; 39:205–212. [PubMed: 10625495]

20. Dillingham MS, Wigley DB, Webb MR. Direct measurement of single-stranded DNA translocation by PcrA helicase using the fluorescent base analogue 2-aminopurine. Biochemistry. 2002; 41:643–651. [PubMed: 11781105]
21. Brendza KM, Cheng W, Fischer CJ, Chesnik MA, Niedziela-Majka A, Lohman TM. Autoinhibition of Escherichia coli Rep monomer helicase activity by its 2B subdomain. Proc Natl Acad Sci U S A. 2005; 102:10076–10081. [PubMed: 16009938]
22. Niedziela-Majka A, Chesnik MA, Tomko EJ, Lohman TM. Bacillus stearothermophilus PcrA monomer is a single-stranded DNA translocase but not a processive helicase in vitro. J Biol Chem. 2007; 282:27076–27085. [PubMed: 17631491]
23. Hsieh J, Moore KJ, Lohman TM. A two-site kinetic mechanism for ATP binding and hydrolysis by E. coli Rep helicase dimer bound to a single-stranded oligodeoxynucleotide. J Mol Biol. 1999; 288:255–274. [PubMed: 10329141]
24. Wong I, Moore KJ, Bjornson KP, Hsieh J, Lohman TM. ATPase activity of Escherichia coli Rep helicase is dramatically dependent on DNA ligation and protein oligomeric states. Biochemistry. 1996; 35:5726–5734. [PubMed: 8639532]
25. Dessinges MN, Lionnet T, Xi XG, Bensimon D, Croquette V. Single-molecule assay reveals strand switching and enhanced processivity of UvrD. Proc Natl Acad Sci U S A. 2004; 101:6439–6444. [PubMed: 15079074]
26. Myong S, Bruno MM, Pyle AM, Ha T. Spring-loaded mechanism of DNA unwinding by hepatitis C virus NS3 helicase. Science. 2007; 317:513–516. [PubMed: 17656723]
27. Myong S, Rasnik I, Joo C, Lohman TM, Ha T. Repetitive shuttling of a motor protein on DNA. Nature. 2005; 437:1321–1325. [PubMed: 16251956]
28. Lu HP, Xun L, Xie XS. Single-molecule enzymatic dynamics. Science. 1998; 282:1877–1882. [PubMed: 9836635]
29. Neuman KC, Abbondanzieri EA, Landick R, Gelles J, Block SM. Ubiquitous transcriptional pausing is independent of RNA polymerase backtracking. Cell. 2003; 115:437–447. [PubMed: 14622598]
30. Bianco PR, Brewer LR, Corzett M, Balhorn R, Yeh Y, Kowalczykowski SC, Baskin RJ. Processive translocation and DNA unwinding by individual RecBCD enzyme molecules. Nature. 2001; 409:374–378. [PubMed: 11201750]
31. Perkins TT, Li HW, Dalal RV, Gelles J, Block SM. Forward and reverse motion of single RecBCD molecules on DNA. Biophys J. 2004; 86:1640–1648. [PubMed: 14990491]

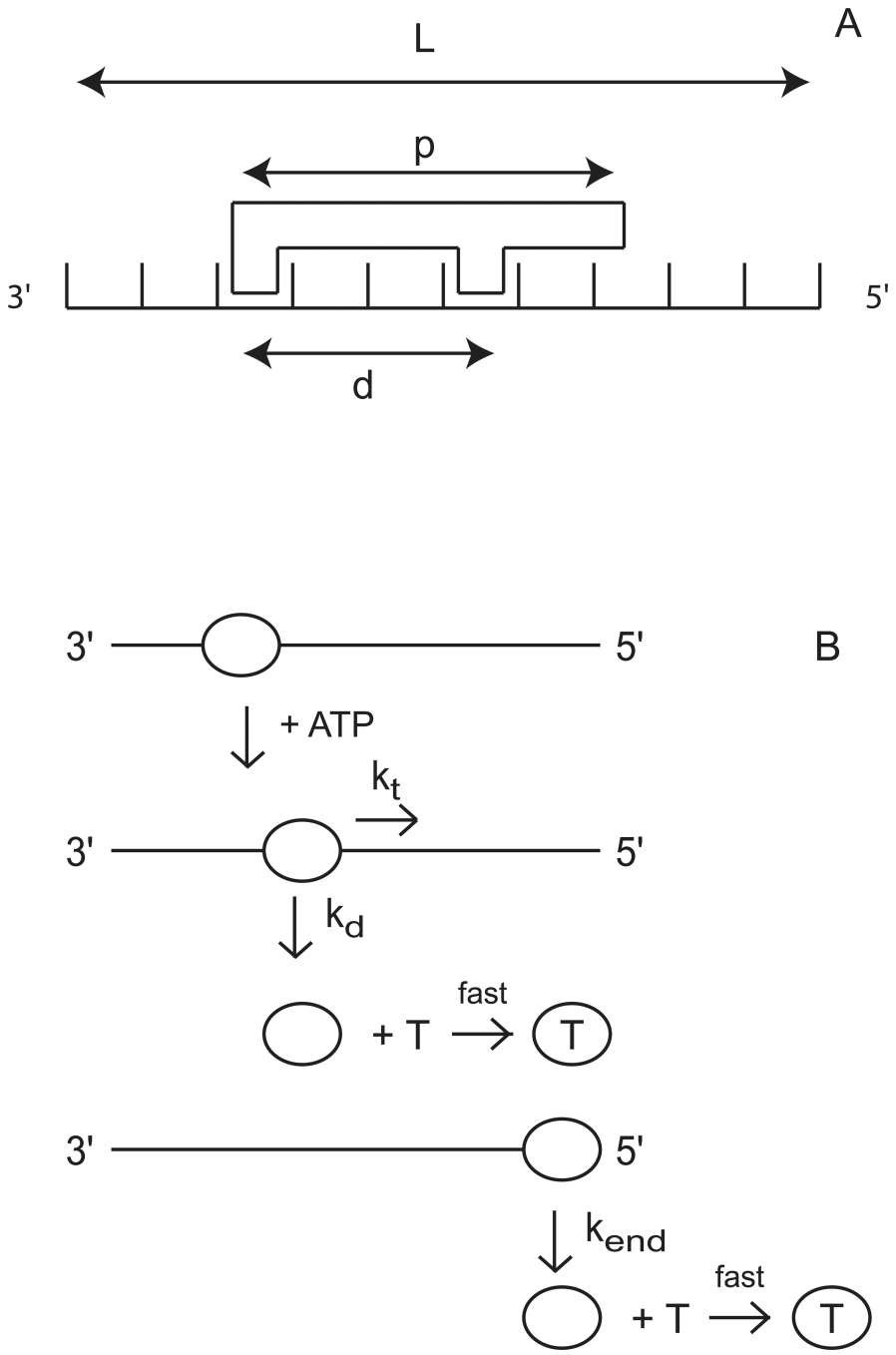

Figure 1.

Kinetic model for ATP-dependent protein translocation along a nucleic acid filament. Panel A: A cartoon depicting the binding of a translocase with a contact size *d* and occluded site size *b* to a nucleic acid filament of length *L*. As shown in this cartoon, the contact size, *d*, is always less than or equal to the occluded site size, *b*. Panel B: Cartoon showing the model used to describe enzyme translocation along a nucleic acid filament. The line segments represent the nucleic acid and the triangles represent the translocase. The translocase binds randomly, but with polarity, to the nucleic acid and upon binding and hydrolysis of ATP proceeds to translocate toward the 5' end of the filament in discrete steps with rate constant k_t. The rate constant of dissociation during translocation is k_d. Upon reaching the 5' end of

the filament, the translocase dissociates with a rate constant k_{end}. Dissociated translocases bind to a protein trap, T, and are thereby prevented from rebinding the nucleic acid.

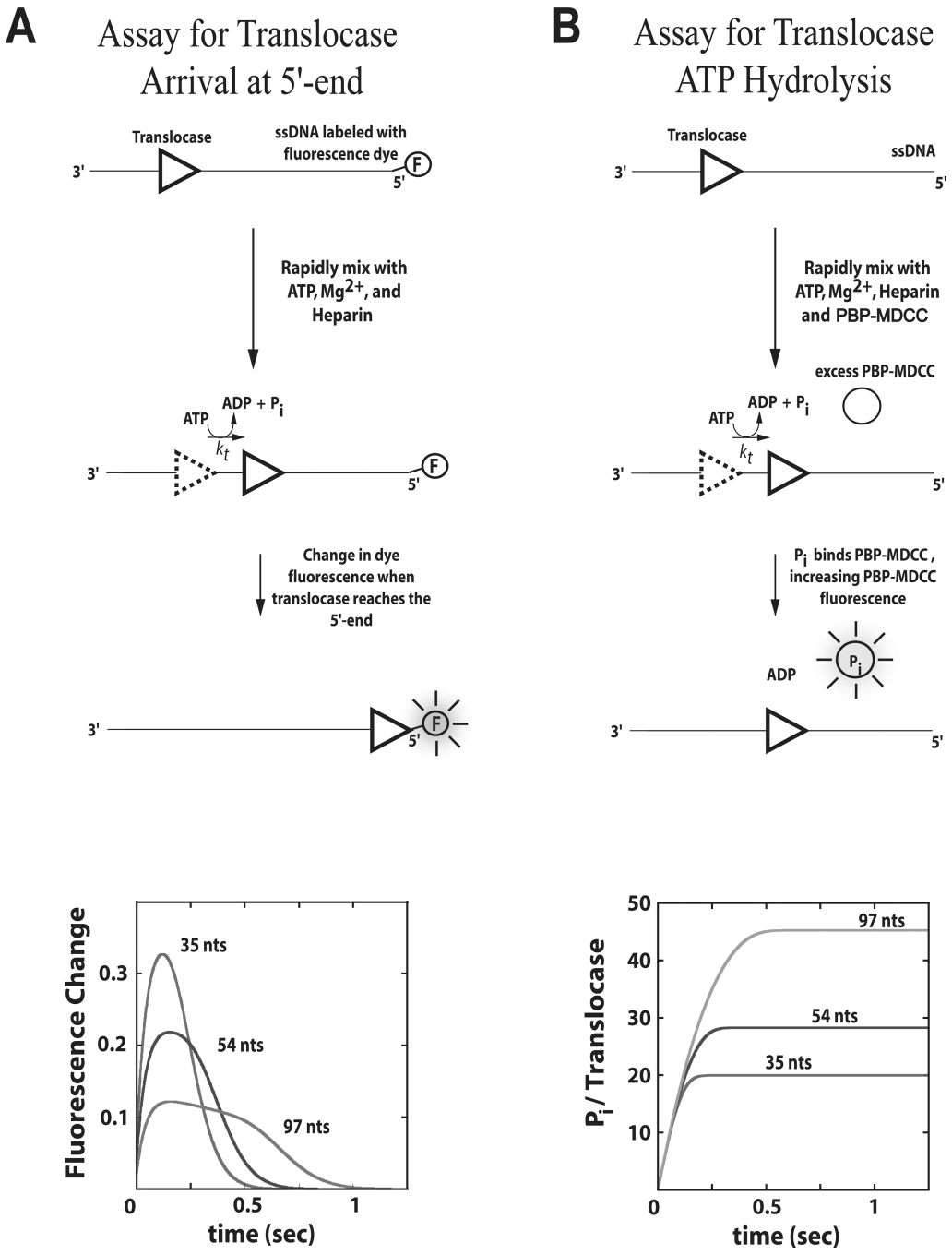

Figure 2.

Stopped-flow assays for monitoring the pre-steady state kinetics of enzyme translocation along nucleic acid filaments. Panel A: A translocase is pre-bound to a nucleic acid filament labeled at the 5'-end with a fluorescent dye, then rapidly mixed with ATP, Mg^{2+}, and heparin (protein trap) to initiate translocation. When the translocase nears the 5'-end of the nucleic acid the fluorescence of the dye is either quenched or enhanced. Example time courses are shown for three different lengths of nucleic acid. Panel B: A translocase is pre-bound to a nucleic acid filament and then rapidly mixed with ATP, Mg^{2+}, heparin, and an excess concentration of fluorescently labeled phosphate binding protein (PBP-MDCC) to initiate translocation. As the translocase moves along the filament, ATP is hydrolyzed into

ADP and inorganic phosphate (P_i). PBP-MDCC rapidly binds the P_i resulting in an increase in the PBP-MDCC fluorescence. Example time courses are shown for three different lengths of nucleic acid.

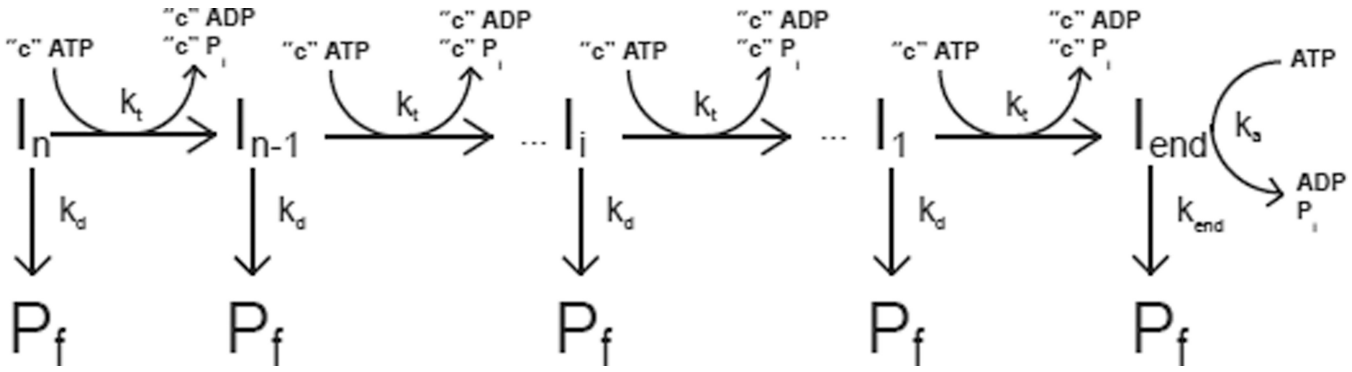

Scheme 1.